Elastic String in a Random Potential

M. Dong, M. C. Marchetti, and A. Alan Middleton
Physics Department, Syracuse University, Syracuse, New York 13244

V. Vinokur
Argonne National Laboratory, Materials Science Division, Argonne, Illinois 60439

(Received 3 January 1992)

We have studied numerically the dynamics of a directed elastic string in a two-dimensional array of quenched random impurities. The string is driven by a constant transverse force and thermal fluctuations are neglected. There is a transition from pinned to unpinned behavior at a critical value F_T of the driving force. At the transition the average string velocity scales with the driving force. The scaling is equally well described by a power law $v_d \sim (F - F_T)^\zeta$, with $\zeta = 0.24 \pm 0.1$, or by a logarithm, $v_d \sim 1/\ln(F - F_T)$. The divergence of the velocity-velocity correlation length at threshold is characterized by an exponent $\nu = 1.05 \pm 0.1$.

PACS numbers: 74.60.Ge, 05.60.+w, 68.10.–m

The effect of disorder on the dynamical properties of a driven elastic medium is of interest for a number of physical situations. These include one-dimensional models of charge density waves (CDW's) [1, 2], flux flow in type-II superconductors [3], and the motion or growth of various linear boundaries between two systems or two phases of the same system, such as the interface of a fluid displacing a second fluid in a porous medium [4]. This model is also closely related to models of friction, earthquakes, and sandpiles [5].

The specific problem considered here is the motion of an elastic string driven by a transverse constant force through a two-dimensional array of randomly distributed pinning centers. The impurities are fixed in time and they provide a type of quenched disorder qualitatively different from the noise in the well-known Kardar-Parisi-Zhang (KPZ) model of interface dynamics, where disorder is uncorrelated in time [6]. Analytical work on the dynamics of the string with quenched disorder has been limited to mean field theory [7, 8] and to perturbation theory in the disorder [7, 9] to analyze the motion at large driving forces. Ioffe and Vinokur discussed the string dynamics for small driving forces and finite temperature [10]. While these asymptotic regimes are rather well understood, the dynamics in the nonperturbative region near threshold needs further investigation.

In this paper we present the results of a numerical study of the motion of the string in the absence of thermal fluctuations. We have found that, as in the CDW model, there is a threshold value of the driving force below which the string is stuck in a pinned configuration and above which the string moves on the average in the direction of the driving force. As discussed below, there are, however, qualitative and quantitative differences between CDW models and the model we study here. We are mainly interested in the behavior just above this depinning transition, where transport is collective and perturbative methods cannot be used. The behavior near threshold is that of a dynamic critical phenomenon and it can be described by scaling laws and critical exponents [8]. We find that the average velocity scales with the reduced driving force $f = (F - F_T)/F_T$. The data are equally well described by a logarithm, $v_d \sim 1/\ln(f)$, or by a power law, $v_d \sim f^\zeta$, with a small exponent $\zeta = 0.24 \pm 0.1$. To gain insight into the behavior near threshold, we have also studied equal-time velocity and position correlation functions. The spatial range of the velocity correlations is determined by a correlation length ξ that diverges near threshold as $\xi \sim f^{-\nu}$, with $\nu = 1.05 \pm 0.1$. We find that the temporal fluctuations around the mean velocity also diverge as threshold is approached, with an exponent consistent with that found from the scaling of the velocity correlations and arguments due to Fisher [8].

The main difference between CDW simulations in one dimension and the model considered here is in the pinning potential. In CDW's the pinning potential is uncorrelated along the length of the string, but is periodic in the direction transverse to the string. Here the pinning potential has short-range correlations both along the string direction and transverse to the string. Because the disorder is uncorrelated, any finite string will eventually encounter a region of exceptionally strong pinning that will stop its motion. However, the expected time to encounter such a region increases exponentially with system size.

The present model is relevant for the motion of magnetic flux lines in the mixed phase of type-II superconductors at moderate fields, as long as intervortex interactions can be neglected [11]. In real systems fluctuations in the direction transverse to the average motion are, however, possible and may play a significant role in the region near threshold. The present study should therefore be considered mainly as the first step towards the study of the dynamics of real interacting flux-line arrays in three dimensions. In addition, the model is relevant for the dynamics of the immiscible-fluid interface in porous media. Some of our results compare favorably with experiments in such systems.

The specific model we have studied is an elastic string embedded in two dimensions and on the average aligned with the z direction (in the superconductor this is the direction of the applied magnetic field). The position of a point on the string at height z and time t is denoted by $x(z,t)$. The Hamiltonian for the string is

$$H = \int_0^L dz \left\{ \frac{K}{2} \left(\frac{\partial x}{\partial z} \right)^2 + \sum_{i=1}^{N_p} U_i(\mathbf{r} - \mathbf{R}_i) - \mathcal{F} x(z) \right\}, \tag{1}$$

where L is the size of the system in the z direction. The first term in Eq. (1) is the elastic energy of the string, with K the string elastic constant. The second term describes the interaction with N_p impurities randomly distributed throughout the plane at positions $\mathbf{R}_i$. Here $\mathbf{r} = (x(z), z)$ denotes a point on the string. The interaction U_i of the string with the ith pin is approximated by a potential well centered at the pin location $\mathbf{R}_i$ with maximum depth U_0 (the depth is the same for all the pins—it is not a random variable) and width R_p in both the x and z directions. The last term in Eq. (1) arises from the constant driving force per unit length $\mathcal{F}$ applied to the string in the x direction.

We consider the overdamped string dynamics. Neglecting thermal fluctuations, the equation of motion for the elastic string is

$$\frac{\partial x}{\partial t} = \frac{\partial^2 x}{\partial z^2} - F_p \sum_{i=1}^{N_p} \frac{\delta(U_i/U_0)}{\delta x} + F, \tag{2}$$

where we have introduced dimensionless variables and parameters. All lengths are measured in units of R_p and time is measured in units of $t_0 = \gamma R_p^2/K$, with γ a friction coefficient. Also $F = \mathcal{F} R_p/K$ is a dimensionless driving force and $F_p = U_0/K$ a dimensionless pinning force.

The overall motion of the string can be described in terms of a "center-of-mass" velocity, defined as

$$v_{\text{c.m.}}(\mathcal{F}, t) = \frac{1}{L} \int_0^L dz\, v(z,t), \tag{3}$$

where $v(z,t) = \partial x/\partial t$ is the instantaneous velocity of a point on the string. The center-of-mass velocity is a fluctuating quantity since it depends on the random positions of the pinning centers. The drift or average velocity of the string is given by

$$v_d(\mathcal{F}) = \langle v_{\text{c.m.}}(\mathcal{F}, t) \rangle, \tag{4}$$

where the angular brackets denote the average over time. In the calculation we average over impurity realizations by performing an average over time since as time evolves the string samples different impurity configurations.

We integrated numerically the discretized version of the equation of motion (2) for strings composed of discrete elements, each of dimensionless size 1 (i.e., R_p) in the z direction, that interact through nearest-neighbor elastic forces. We imposed periodic boundary conditions in the z direction. Each element is subject to an x- and z-dependent pinning potential consisting of randomly distributed triangular wells of width 1. We have run simulations for two values of the well depth, $U_0 = 0.05$ ($F_p = 0.1$) and $U_0 = 0.5$ ($F_p = 1$); the density of pins was chosen be $\rho = n_p R_p^2 = 0.1$, while the elastic constant was unity. The first set of parameters ($F_p = 0.1$) lies at the crossover between weak and strong pinning regimes according to a dimensional estimate of the condition for weak pinning, $\rho > F_p$. By examining string configurations as a function of time it appears, however, that this choice of parameters corresponds to weak pinning. The second set of parameters ($F_p = 1$) lies in the strong pinning regime. As the pinning force is discontinuous, we used a simple Euler algorithm for the simulation and chose a time step small enough (typically $\Delta t = 0.1$) that the results were insensitive to doubling the time step. For fields within 10% of threshold, the length of the simulation usually exceeded 4×10^7 time steps, while for fields further from threshold, shorter simulation times gave very good averages. We investigated systems of sizes from 256 to 16 384.

For $F_p = 1$ the transition from the pinned to the unpinned regime occurs at a critical value $F_T = 0.3058 \pm 0.0002$ of the driving force, as shown in Fig. 1. This value is of the order given by a dimensional estimate, $F_T = \rho F_p$, which gives $F_T = 0.1$. For $F_p = 0.1$ the depinning transition takes place at $F_T \simeq 0.015\,05$. This value is consistent with the dimensional estimate of F_T for both strong ($F_T = \rho F_p$) and weak ($F_T = \rho^{2/3} F_p^{4/3}$) pinning, since they both give $F_T = 0.01$. For large driving forces, $F \gg F_T$, the effects of pinning are negligible and the string advances uniformly, with $v_d \approx F$. The

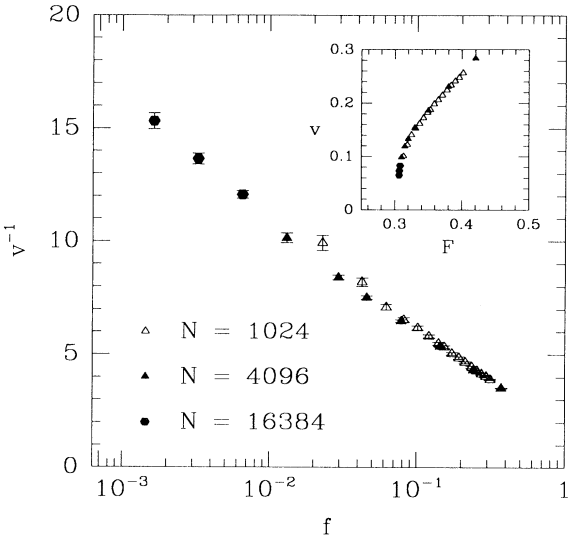

FIG. 1. The scaling of the drift velocity $v_d \sim 1/\ln(f)$ for $F_p = 1$ and various system sizes. Inset: v_d vs F to highlight the depinning transition.

deviations from this asymptotic form were studied by a perturbation expansion in F/F_p [2, 9], with the result $v_d/F = 1 - CF^{-3/2}$, in agreement with our simulations [12]. As the driving force F is lowered towards the threshold value the motion of the string becomes more and more jerky. Near threshold the perturbation theory breaks down. The scaling of the average velocity with reduced driving force is well described by $v_d \sim 1/\ln(f)$ or by a power law, $v_d \sim f^{\zeta}$, with a small exponent ($\zeta = 0.24 \pm 0.1$ for $F_p = 1$ and $\zeta = 0.34 \pm 0.1$ for $F_p = 0.1$). The strong pinning data are shown in Fig. 1. One may expect that the scaling exponents near threshold should be the same for weak and strong pinning since they describe behavior of the string at large length scales. At present our results do not answer this question conclusively. The scaling exponents obtained for the two values of the pinning force are consistent within experimental error, but more work is needed to properly address this point.

In both weak and strong pinning regimes there is a correlation length ξ that diverges at threshold as $\xi \sim f^{-\nu}$, with ν the correlation length exponent. Away from threshold ξ has the bare value ξ_0 and is the smallest length scale over which the shape of the string varies, $\xi_0 \sim l_p = (F_p\sqrt{\rho})^{-2/3}$ for weak pinning and $\xi_0 \sim 1/\rho$ for strong pinning. Near threshold the string can get stuck for some time in a region where pinning forces roughly balance the driving force: a section of the string is coherently pinned and its velocity vanishes. After a while the string moves forward and jumps to a new configuration. This behavior is displayed in Fig. 2, showing maps of the local velocity of the string. White regions are regions of zero velocity, while dark regions are regions where the velocity is largest. The stationary pinned regions become very large near threshold. The correlation length ξ is related to the linear dimension of these regions through the exponents η and κ discussed below.

When the string is in a sliding state (i.e., one with $v_d \neq 0$) the center-of-mass velocity $v_{\text{c.m.}}(t)$ exhibits fluctuations in time that become large near threshold. To analyze the velocity fluctuations we have considered the rms velocity, $v_{\text{rms}} = \sqrt{\langle [v_{\text{c.m.}}(t)]^2\rangle - \langle v_{\text{c.m.}}(t)\rangle^2}$. After initial transients, the probability of observing a given velocity at any time is fitted well by a Gaussian shape, with mean $\langle v_{\text{c.m.}}\rangle$ and standard deviation v_{rms} (note that in CDW models, distinct samples will have differing v_{rms}). This supports our expectation that the time to stopping due to rare regions grows exponentially with the system size. Just above the transition from pinned to unpinned behavior, where the velocity is small, the velocity fluctuations are of the same size as the velocity itself. Naively the magnitude of the rms noise relative to the average velocity is expected to scale as the number of correlation lengths in the sample, $v_{\text{rms}}/v_d \sim (\xi/L)^{1/2}$. On the other hand, velocity correlations are not perfectly coherent within a length ξ [8]. As a result the effective coherence length that determines the rms noise may be smaller than ξ and $v_{\text{rms}}/v_d \sim (\xi^{4-\eta}/L)^{1/2}$. Here $4 - \eta$ can be thought of as an effective dimensionality, with $4 - \eta \leq d$ and d the dimensionality (here $d = 1$). Using $\xi \sim f^{-\nu}$, our results for the ratio v_{rms}/v_d are well described over more than two decades in reduced field and a factor of 16 in system size by this form with $\nu(4 - \eta)/2 = 0.5 \pm 0.05$ for both $F_p = 0.1$ and $F_p = 1$.

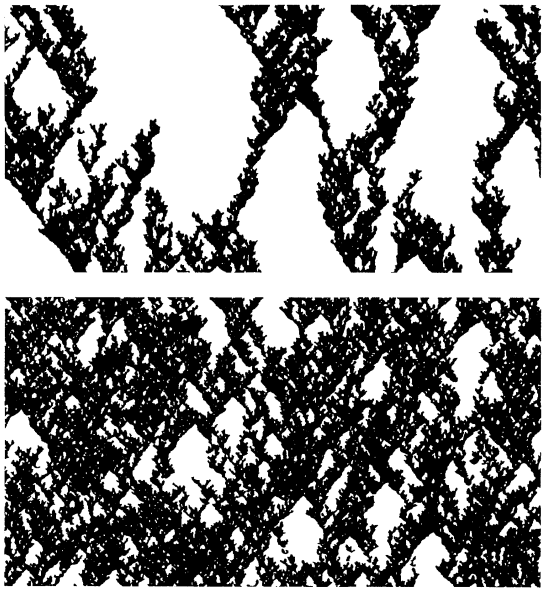

FIG. 2. Maps of string velocity for $f = 0.01$ (top) and $f = 0.076$ (bottom) and $F_p = 0.1$. The vertical axis is time, while the horizontal axis is the position z on the string. Dark regions indicate where the velocity exceeds 0.01. Maps are shown for strings of size $L = 4096$ evolving over a time interval $\Delta t = 30$.

Above threshold the correlation length ξ characterizes the decay of velocity fluctuations. The equal-time velocity correlation function is defined as

$$C_v(z) = \langle \overline{v(z,t)v(0,t)}\rangle - \langle [\overline{v}(t)]^2\rangle, \tag{5}$$

where the overbar denotes the spatial average over the length of the string. We find that velocity correlations scale with ξ according to $C_v(z)/v_d^2 \sim \xi^{4-\eta-1}G_v(z/\xi)$ [8], with $\nu = 1.05 \pm 0.1$ and $\eta = 3.12 \pm 0.1$, consistent with the results obtained for ν and η from the rms noise, as required by $(1/L)\int_0^L dz\, C_v(z) = v_{\text{rms}}^2$. The scaling of velocity correlations is shown in Fig. 3 for $F_p = 1$. The figure also shows that the decay of correlations within a length ξ is fitted by a power law over more than two decades, i.e., $G_v \sim z^{-\kappa}$, with $\kappa = 0.5 \pm 0.05$. A power-law decay of velocity correlations was also reported by Sibani and Littlewood [13] for CDW's. Much longer simulation lengths are required for the convergence of the data at the smaller value of the pinning force ($F_p = 0.1$). At present the evidence for power-law decay of velocity correlations

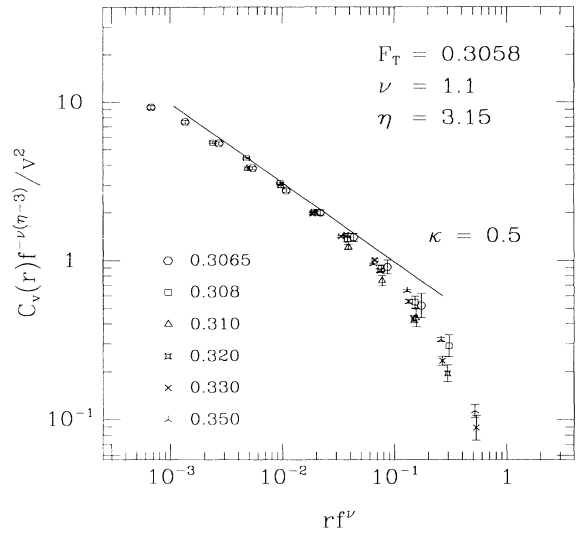

FIG. 3. The velocity correlation functions $C_v(z)/v_d^2$ for $F_p = 1$ and six different values of f collapse on one curve when scaled as described in the text. The straight line shows the power-law decay of the correlations at short distances, $C_v \sim z^{-\kappa}$, with $\kappa = 0.5$.

in this case is not as good as for the data displayed in Fig. 3.

To analyze the distortion of the string configuration under the competing action of disorder and elasticity, we have evaluated the correlation function of the transverse positions of points on the string at a distance z,

$$C_x(z) = \langle \overline{[x(z) - x(0)]^2} \rangle. \quad (6)$$

The size $l_\perp(z)$ of the transverse fluctuations of a length z of string is $l_\perp(z) = \sqrt{C_x(z)}$. Near threshold, where the correlation length ξ is of the order of the system size, we find that the transverse correlation length $l_\perp(z)$ scales as $l_\perp(z) \sim z^\chi$, with $\chi = 0.97 \pm 0.05$ for both pinning strengths. Since χ is near 1, linear elasticity theory is marginally self-consistent, in contrast with one-dimensional CDW models [14]; the strain will become large only in exponentially rare regions. Away from threshold ξ is smaller than the system size and there is a crossover from a regime where $l_\perp(z) \sim z^\chi$, for $z < \xi$ to a regime where $l_\perp(z) \sim z^{1/2}$, for $z \gg \xi$. The asymptotic scaling behavior is therefore that of the KPZ equation. On smaller length scales, however, quenched noise broadens the interface. A similar crossover has been observed in experiments on the roughening of the interface that forms when a fluid displaces another in a porous medium [4]. These experiments show a crossover from $\chi \simeq 0.81$ at short length scales to $\chi \simeq 0.49$ at large length scales. Values of χ in the range $0.5 - 1$ have also been obtained for stochastic growth models for the propagation of an interface [15].

This work was conducted using the computational resources of the Northeast Parallel Architectures Center (NPAC) at Syracuse University. It was supported at Syracuse by the National Science Foundation through Grants No. DMR87-17337 and No. DMR91-12330. V.V. acknowledges support through the U.S. Department of Energy, BES–Materials Sciences, under Contract No. W-31-109-ENG-38, and through the NSF funded Science and Technology Center for Superconductivity under Grant No. DMR88-09854.

[1] H. Fukuyama and P.A. Lee, Phys. Rev. B **17**, 535 (1977); P.A. Lee and T.M. Rice, Phys. Rev. B **19**, 3970 (1979).
[2] L. Sneddon, M.C. Cross, and D.S. Fisher, Phys. Rev. Lett. **49**, 292 (1982).
[3] A.I. Larkin and Y.N. Ovchinnikov, J. Low Temp. Phys. **34**, 409 (1979); M.B. Feigel'man and V.M. Vinokur, Phys. Rev. B **41**, 8986 (1990).
[4] V.K. Horváth, F. Family, and T. Vicsek, J. Phys. A **24**, L25 (1991).
[5] P. Bak, C. Tang, and K. Wiesenfeld, Phys. Rev. Lett. **59**, 381 (1987).
[6] M. Kardar, G. Parisi, and Y. Zhang, Phys. Rev. Lett. **56**, 889 (1986).
[7] J. Koplik and H. Levine, Phys. Rev. B **31**, 1396 (1985).
[8] D.S. Fisher, Phys. Rev. B **31**, 1396 (1985).
[9] M.V. Feigel'man, Zh. Eksp. Teor. Fiz. **85**, 1851 (1983) [Sov. Phys. JETP **58**, 1076 (1983)].
[10] L.B. Ioffe and V.M. Vinokur, J. Phys. C **20**, 6149 (1987).
[11] The part of the (H,T) phase diagram where single-flux-line dynamics is relevant extends above H_{c1} in a region where the driving current can be considered uniform, as discussed for instance in M.V. Feigel'man and V.M. Vinokur, Phys. Rev. B **41**, 8986 (1990). This is because the crossover from the single-vortex regime to the collective pinning regime where the dissipation takes place via the motion of correlated flux bundles is estimated to occur when the intervortex spacing is comparable to the in-plane Larkin-Ovchinnikov pinning length, which is typically much shorter than the penetration length.
[12] This correction is strictly correct only at intermediate fields. At very high fields, there is a crossover to the single-particle behavior $1 - v/F \sim F^{-2}$ that depends on the range of the potential correlations in the z direction. We see the latter behavior at fields 100 times larger than the depinning field.
[13] P. Sibani and P. B. Littlewood, Phys. Rev. Lett. **64**, 1305 (1990).
[14] S. N. Coppersmith, Phys. Rev. Lett. **65**, 1044 (1990); S. N. Coppersmith and A. J. Millis, Phys. Rev. B **44**, 7799 (1991).
[15] E. Medina, T. Hwa, M. Kardar, and Y.-V. Zhang, Phys. Rev. A **39**, 3053 (1989); D.A. Kessler, H. Levine, and Y. Tu, Phys. Rev. A **43**, 4551 (1991).